DMD Fast Forward. Published on June 29, 2018 as DOI: 10.1124/dmd.118.082008
This article has not been copyedited and formatted. The final version may differ from this version.

Glycyrrhizin alleviates non-alcoholic steatohepatitis via modulating bile acids and meta-inflammation

Tingting Yan, Hong Wang, Lijuan Cao, Qiong Wang, Shogo Takahashi, Tomoki Yagai, Guolin Li, Kristopher W. Krausz, Guangji Wang, Frank J. Gonzalez, Haiping Hao.

Author Affiliations:

State Key Laboratory of Natural Medicines, Key Laboratory of Drug Metabolism and Pharmacokinetics, China Pharmaceutical University, Nanjing, Jiangsu 210009, China (Ti. Y., H.W., L.C., G.W., H.H.) and Laboratory of Metabolism, Center for Cancer Research, National Cancer Institute, National Institutes of Health, Bethesda, MD 20892 (Ti. Y., Q.W., S.T., T.Y., G.L., K.W.K., F.J.G.).

DMD Fast Forward. Published on June 29, 2018 as DOI: 10.1124/dmd.118.082008
This article has not been copyedited and formatted. The final version may differ from this version.

Running Title: Glycyrrhizin improves non-alcoholic steatohepatitis

Correspondence:

☒Frank J. Gonzalez, Laboratory of Metabolism, Center for Cancer Research, National Cancer Institute, National Institutes of Health, Bethesda, MD 20892, USA. gonzalef@mail.nih.gov;

☒ Haiping Hao, State Key Laboratory of Natural Medicines, Key Laboratory of Drug Metabolism and Pharmacokinetics, China Pharmaceutical University, No.24, Tongjiaxiang, Nanjing 210009, China; haipinghao@cpu.edu.cn.

Number of text pages:46

Number of tables:0

Number of figures:7

Number of references:40

Words of Abstract:219

Words of Instruction:647

Words of Discussion: 795

Abbreviations:

Acat1, acetyl-CoA acetyltransferase 1; ACTD, actinomycin D; ALT, Alanine aminotransferase; AST, aspartate aminotransferase; ASC, apoptosis-associated speck like protein containing a caspase recruitment domain; Bsep, bile salt export pump; CA, cholic acid; CASP1, caspase 1;

Cola, collagen; DAMPs; damage-associated molecular patterns; DCA, deoxycholic acid; FACS, fluorescence-activated cell sorting; Fatp, fatty acid transport protein; FXR, farnesoid X receptor; Gapdh, glyceraldehyde 3-phosphate dehydrogenase; G-CA, glycocholic acid; GA 30, GA 30 mg/kg; GA, glycyrrhetinic acid; GL, glycyrrhizin; GL50, glycyrrhizin 50 mg/kg; HDCA, hyodeoxycholic acid; HDL, high-density lipoprotein; H&E, hematoxylin and eosin; Hmgcl, 3-hydroxy-3-methylglutaryl-CoA lyase; Hmgcs, hydroxymethylglutaryl-CoA synthase; Il1b, interleukin 1b; Il6, interleukin 6; PAMPs, pathogen-associated molecular patterns; Ppara, peroxisome proliferator-activated receptor alpha; qPCR, quantitative polymerase chain reaction; SHP, small heterodimer partner; LCA, lithocholic acid; LDL, low-density lipoprotein; LPS, lipopolysaccharide; LRH, liver receptor homolog; LXR, liver X receptor; MCA, muricholic acid; MCD, methionine-choline-deficient; MCS, methionine-choline-sufficient; Mmp, matrix metalloproteinase; Myd88, myeloid differentiation primary response 88; NAFLD, non-alcoholic fatty liver disease; NAS, non-alcoholic steatosis; NASH, non-alcoholic steatohepatitis; NLRP3, NLR family, pyrin domain-containing 3; Scd1, Stearoyl-CoA desaturase 1; Srebp1, sterol regulatory element-binding transcription factor 1; TC, total cholesterol; TCM, traditional Chinese medicine; T-CA, taurocholic acid; T-CDCA, taurochenodeoxycholic acid; T-DCA, taurodeoxycholic acid; TG, triglyceride; Tgfb1, transforming growth factor beta-1; T-HDCA, taurohyodeoxycholic acid; Timp, tissue inhibitor of metalloproteinases; TLR, toll-like receptor; T-β-MCA, tauro-β-muricholic acid; TNF, tumor necrosis factor; T-UDCA, tauroursodeoxycholic acid; TUNEL, terminal deoxynucleotidyl transferase-mediated dUTP nick end labeling; UDCA, ursodeoxycholic acid.

DMD Fast Forward. Published on June 29, 2018 as DOI: 10.1124/dmd.118.082008
This article has not been copyedited and formatted. The final version may differ from this version.

ABSTRACT

Non-alcoholic steatohepatitis (NASH) is the progressive stage of non-alcoholic fatty liver disease that may ultimately lead to cirrhosis and liver cancer, and there are few therapeutic options for its treatment. Glycyrrhizin (GL), extracted from the traditional Chinese medicine (TCM) liquorice, has potent hepatoprotective effects in both preclinical animal models and in humans. However, little is known about its effects and mechanisms in treating NASH. To explore the effects of GL on NASH, GL or its active metabolite glycyrrhetinic acid (GA), was administered to mice treated with a methionine-choline-deficient (MCD) diet-induced NASH model, and histological and biochemical analyses used to measure the degree of lipid disruption, liver inflammation and fibrosis. GL significantly improved MCD diet-induced hepatic steatosis, inflammation and fibrosis, and inhibited activation of the NLR family pyrin domain-containing 3 (NLRP3) inflammasome. GL significantly attenuated serum bile acids accumulation in MCD diet-fed mice partially by restoring inflammation-mediated hepatic farnesoid X receptor (FXR) inhibition. In Raw 264.7 macrophage cells, both GL and GA inhibited deoxycholic acid-induced NLRP3 inflammasome-associated inflammation. Notably, both intraperitoneal injection of GL's active metabolite GA, and oral administration of GL, prevented NASH in mice, indicating that GL may attenuate NASH via its active metabolite GA. These results reveal that GL, via restoring bile acids homeostasis and inhibiting inflammatory injury, can be a therapeutic option for treatment of NASH.

DMD Fast Forward. Published on June 29, 2018 as DOI: 10.1124/dmd.118.082008
This article has not been copyedited and formatted. The final version may differ from this version.

Introduction

Non-alcoholic fatty liver disease (NAFLD) affects 25% of the global adult population, and has become a leading cause of chronic liver disease in the Western countries and increasingly affects the Asian population (Younossi et al., 2016). Early stage NAFLD is asymptomatic, however, when NAFLD progresses to non-alcoholic steatohepatitis (NASH), patients have a high risk of adverse events including fibrosis, cirrhosis, and NASH-driven hepatocellular carcinoma (Wong et al., 2014; Wong et al., 2016; Zoller and Tilg, 2016). Traditional Chinese medicine (TCM) has been investigated for treating NASH (Jadeja et al., 2014; Zhang and Schuppan, 2014). Glycyrrhizin (GL) is a potent hepatoprotective constituent extracted from TCM liquorice as revealed by various animal experimental liver injury models (Li et al., 2014; Yan et al., 2016), and thus is clinically used for treating chronic liver diseases in some Asian countries (Li et al., 2014). Clinical prescription preference for GL is found mainly for treating chronic liver diseases especially for viral hepatitis in China and Japan (Li et al., 2014), while the preclinical studies of GL in treating liver diseases mostly focused on viral hepatitis and drug/toxins-induced hepatotoxicity (Li et al., 2014; Yan et al., 2016; Zhou et al., 2016). However, the effect of GL in preventing NASH is largely unknown. Until now, only glycyrrhetinic acid (GA), the metabolite of GL *in vivo*, was found to prevent high-fat diet-induced NAFLD in rats *in vivo* and free fatty acids-induced toxicity in HepG2 cells *in vitro* (Wu et al., 2008). Whether and how GL and GA affect NASH, the progressive stage of NAFLD, is still unknown.

DMD Fast Forward. Published on June 29, 2018 as DOI: 10.1124/dmd.118.082008
This article has not been copyedited and formatted. The final version may differ from this version.

Bile acids homeostasis, which is mainly modulated by FXR, is disrupted in experimental NASH mouse models and clinical human NASH patients (Arab et al., 2017). Dysregulated bile acids disruption correlates with Non-alcoholic steatosis (NAS) score in obese NAFLD (Bechmann et al., 2013), causes cholestatic liver injury (Schoemaker et al., 2003), and promotes liver carcinogenesis in NASH-driven hepatocellular carcinoma model in mice (Xie et al., 2016). Furthermore, a bile acid sequestrant was found to prevent NAFLD and NASH (Arab et al., 2017), suggesting that to suppress the accumulation of bile acids during NASH could benefit NASH treatment. On the other hand, the NLRP3 inflammasome is known to be required for hepatocyte pyroptosis, liver inflammation, and fibrosis development in NAFLD (Wree et al., 2014a; Wree et al., 2014b). Metabolic homeostasis is associated with the immune system (Osborn and Olefsky, 2012), among which several bile acids were recently demonstrated to directly activate the NLRP3 inflammasome (Hao et al., 2017), providing a link between immune dysfunction with metabolic disorder. Since bile acids accumulate in NASH livers, it is reasonable to infer that toxic bile acids induced NLRP3 inflammasome activation and could be a key factor in mediating NASH progression. Bile acids-NLRP3 inflammasome axis is a potential pharmacological target for treating NASH.

GL was demonstrated to inhibit lithocholic acid (LCA)-induced cholestatic liver injury (Wang et al., 2012), bile acid-induced cytotoxicity in rat hepatocytes (Gumpricht et al., 2005) as well as alpha-naphthyl isothiocyanate-induced liver injury and bile acids disruption (Wang et al., 2017), indicating a potential role for GL in treating cholestatic liver injury. Additionally,

glycyrrhizin is also an inhibitor of NLRP3 inflammasome activation in macrophage *in vitro* and NLRP3 inflammasome-associated adipose tissue inflammation in mice (Honda et al., 2014). Thus, GL might target bile acids-NLRP3 inflammasome to elicit its hepatoprotective function for decreasing NASH.

In this study, the methionine-choline deficient (MCD) diet-induced NASH mouse model was used to examine the hepatoprotective effect and potential mechanisms of GL. GL was found to potently inhibit MCD diet-induced liver lipids accumulation, inflammation, and fibrosis. GL dampened the activation of NLPR3 inflammasome and restored bile acids homeostasis. Moreover, GL also directly inhibited deoxycholic acid-induced NLRP3 inflammasome activation. GL gavage as well as GA significantly prevented MCD diet-induced liver injury, suggesting GL by oral intake might be applied in the clinic as a therapeutic option for NASH patients.

DMD Fast Forward. Published on June 29, 2018 as DOI: 10.1124/dmd.118.082008
This article has not been copyedited and formatted. The final version may differ from this version.

Methods and Materials

Chemicals and Reagents

GL (97%) was purchased from TCI (Shanghai, China). 18β-GA (97%), actinomycin D (ACTD), Tween 80 and lipopolysaccharides (LPS) from Escherichia coli O111:B4 were purchased from Sigma (USA). Recombinant human TNF-α was purchased from R&D (Cat. No. 210-TA, MN, USA). MCD diet and MCS diet were purchased from Trophic Animal Feed High-Tech Co., Ltd (Nantong, China) or Dyets Inc (Bethlehem, PA, USA). The In situ cell death detection kit was purchased from Roche (USA).

Experimental Animals and Treatments

6- to 8-week-old male C57BL/6 mice were obtained from Academy of Military Medical Sciences, China or the National Institutes of Health. Mice were acclimatized to the facilities for a week and then randomly divided into different groups. The animal room was maintained at 25 ± 2 ℃ with a 12-h light-dark cycle and 50 ± 10 % humidity. All animal studies were approved by the Animal Ethics Committee of China Pharmaceutical University and carried out in accordance with the Guide for the Care and Use of Laboratory Animals, National Institutes of Health.

To assess the influence of GL in treating NASH, mice were randomly divided into 4 groups with different treatments for 8 weeks: MCS group (saline, I.P.), MCS+GL50 group (50 mg/kg/day GL, I.P.), MCD group (saline, I.P.), and MCD+GL50 group (50 mg/kg/day GL, I.P.).

All animals were fed MCD or MCS diet for 6 weeks, and then injected with 50 mg/kg/day of GL for two consecutive weeks, while mice were fed matched MCD diet or MCS diet for the last two weeks until the end of experiments. All mice were fasted for 4 hours with free access to water before killing. For testing the effects of GA injection in preventing NASH, mice were divided into 3 groups with different treatments for 6 weeks: MCS group (MCS diet feeding, saline, I.P.), MCD group (MCD diet feeding, 5% Tween 80/saline, I.P.), and MCD+GA30 group (MCD diet feeding, 30 mg/kg/day of GA, dissolved in 5% Tween 80/saline, I.P.). Similarly, in the study for testing the effect of GL gavage, 3 groups of mice were treated accordingly: MCS group (MCS diet feeding, saline, I.P.), MCD group (MCD diet feeding, saline, P.O.), and MCD+GL50 group (MCD diet feeding, 50 mg/kg/day of GL, P.O.). All mice were fed MCD or MCS diet for 6 weeks, and injected with control vehicle or 50 mg/kg/day of GL gavage for the last 3 consecutive weeks, respectively. All mice were killed with CO_2 asphyxiation, and blood and livers were collected and stored for further use. GL was dissolved in saline and pH value adjusted to 7.0-7.5 with 1M sodium hydroxide (NaOH) solution (Sigma). GA was freshly dissolved in saline containing 5% Tween 80.

Histology Analysis

Formalin-fixed liver tissues were embedded in paraffin and 5 μm thick sections were cut for H&E staining, TUNEL staining, and Masson's Trichrome Staining based on respective manual protocol. A portion of fresh livers were embedded in Tissue-Tek Optimal Cutting Temperature (O.C.T.) compound (Sakura Finetek, Torrance, USA) and then flash frozen for

Oil Red O staining. Further samples processing and analysis for Figure 1-3 was performed in the department of Pathophysiology in Affiliated Hospital of Nanjing University of Chinese Medicine (Nanjing, Jiangsu, China) and Figure 7 at Histoserv Inc. (Germantown, MD, USA).

Targeted Bile Acids Metabolome Analysis

The levels of main bile acid species were determined by high-performance liquid chromatography-quadrupole time-of-flight tandem mass spectrometry (UPLC-triple/TOF-MS) as described previously (Hao et al., 2017).

In Vitro Cell Culture and Treatment

Human HepG2 cells were obtained from the American Type Culture Collection (Manassas, VA, USA). For testing the protective effects of GL or GA on ACTD/TNF-α-induced HepG2 cell death, HepG2 cells were seeded in 96-well plates for cell viability assays or 6-well plates for FACS assays and then grown to 70%-90% confluence before use. HepG2 cells were pretreated with control DMSO, GL or GA together with 0.3 μM of ACTD for 30 min, and then treated with recombinant human TNF-α for additional 13 h or 24 h for cell viability assays with the Cell Counting Kit -8 (CCK-8, Dojindo Laboratories, Kumamoto, Japan). For FACS assays, samples were collected at 13 h after treatment and analyzed according to the manufacturer's instruction for the Annexin V FITC apoptosis detection kit (BD Biosciences, San Diego, CA).

Reporter Luciferase Assay

DMD Fast Forward. Published on June 29, 2018 as DOI: 10.1124/dmd.118.082008
This article has not been copyedited and formatted. The final version may differ from this version.

The PGL4-Shp-TK firefly luciferase construct and human FXR expression plasmid were provided by Grace L. Guo (Rutgers University). A *Renilla* luciferase reporter gene (pRL-luciferase; Promega; Madison, WI) was used as a transfection efficiency control. The plasmids were transfected into HepG2 cells that were cultured in 10% Roswell Park Memorial Institute 1640 (RPMI 1640) medium and seeded in 24-well plates at a confluency of 70%-90%. Cells were transfected with plasmids using lipofectamine 3000 reagent (Invitrogen, Thermo Fisher Scientific, MA, USA) for 24 h, and then treated with LPS, GL or GA for another 24 h. The cells were lysed and luciferase activities measured with the Dual Luciferase Reporter Assay kit (Promega Corp., Madison, WI) and a Tecan Genios Pro luminescence plate reader (Research Triangle Park, NC).

Serum Biochemical Analysis

Biochemical parameters including ALT levels, AST levels, total cholesterol (TC) levels, triglyceride (TG) levels, low-density lipoprotein cholesterol (LDL-cholesterol) and high-density lipoprotein cholesterol (HDL-cholesterol) in serum, TC levels and TG levels in liver were quantified using a standard clinical automatic analyzer at Zhongda Hospital Affiliated to Southeastern University.

Western Blot Analysis

Liver samples were lysed in RIPA Lysis Buffer (Millipore, Temecula, California, USA) with protease and phosphatase inhibitors (Halt Protease and Phosphatase Inhibitor Cocktail, Cat #78446, Thermo Scientific, Rockford, USA), and then the protein extracts were separated

by sodium dodecyl sulfate-polyacrylamide gel electrophoresis and transferred to a polyvinylidene difluoride membrane. The membrane was incubated overnight at 4 ℃ with antibodies against mouse β-ACTIN (Cell Signaling, Danvers, MA, Cat#4970), mouse monoclonal anti-caspase 1 (Santa Cruz, Cat#sc-56036), and rabbit polyclonal anti-IL-1β (Santa Cruz, Cat#sc-7884).

Elisa of Serum IL-1β Level in Mice

An IL-1β ELISA kit was purchased from R&D systems (Cat#, MLB00C, MN, USA). Fifty μL of serum was used for analysis based on the manual protocol accordingly.

Quantitative Polymerase Chain Reaction

Total tissue RNA extraction was performed by using the RNAiso Plus reagent (Takara, Bio-Tech Co., Ltd, Dalian, China). Purified total RNA was reverse-transcribed using the Prime Script RT Reagent Kit (Takara Biotechnology Co., Ltd.). Quantitative polymerase chain reaction (qPCR) was performed by using the ABI PRISM 7000 Sequence Detection System (Applied Biosystems, Bedford, MA) and Sybr Green reagent kit (Bio-Rad Co., Ltd., Shanghai, China). Values were normalized to *Gapdh*. Sequences for qPCR primers could be provided upon request.

Statistical analysis

Data are presented as means ± SD. Statistic differences between experimental groups were determined by two-tailed Student's *t* test or one-way ANOVA followed by Dunnett's multiple

DMD Fast Forward. Published on June 29, 2018 as DOI: 10.1124/dmd.118.082008
This article has not been copyedited and formatted. The final version may differ from this version.

comparisons test in GraphPad Prism 7.0 as stated (GraphPad Software Inc., San Diego, CA). P value less than 0.05 was considered statistically significant.

DMD Fast Forward. Published on June 29, 2018 as DOI: 10.1124/dmd.118.082008
This article has not been copyedited and formatted. The final version may differ from this version.

Results

GL attenuates NASH-induced liver injury

To determine whether GL attenuates MCD diet-induced liver injury *in vivo*, C57BL/6 mice were treated with GL after MCD diet feeding for 6 weeks, and the GL treatment continued for the last two weeks while the mice were fed matched MCD diet or MCS diet during the injection (Figure 1A). GL treatment did not significantly affect food intake and body weight (Supplemental Figure 1, A and B) as well as liver index (Supplemental Figure 1C) both in MCS diet-fed mice and MCD diet-fed mice. H&E staining data showed that 50 mg/kg of GL sharply decreased hepatic steatosis in MCD diet-fed mice, while 50 mg/kg of GL treatment alone did not cause liver toxicity (Figure 1B). Apoptotic hepatocyte death is known to be involved in NASH (Feldstein et al., 2003), and therefore liver tissues were analyzed by TUNEL staining to measure apoptosis. GL treatment significantly reduced the positive staining when compared with control saline treatment in MCD diet-fed mice (Figure 1C). Consistently, the apoptosis marker gene mRNA, *Bcl2a1c*, was also significantly inhibited by GL treatment in MCD diet-fed mice (Supplemental Figure 1D). Since TNF-α is an inducer of apoptosis (Wang et al., 1996), and ACTD/TNF-α is frequently used to mimic apoptotic cell death (Leist et al., 1994), the effects of GL in alleviating ACTD/TNF-α-induced apoptosis were examined in HepG2 cells. GL directly inhibited ACTD/TNF-α-induced decrease of cell viability at both 13 h and 24 h after ACTD/TNF-α treatment (Supplemental Figure 1, E and F), and ameliorated the increase in apoptotic cell death as assessed by FACS assay (Supplemental Figure 1G), supporting that

GL could directly inhibit TNF-α-mediated apoptosis. In addition, serum ALT levels were increased in MCD diet-fed group, while they were markedly decreased in the MCD+GL50-treated group (Figure 1D). NAFLD scores among the MCS, MCD and MCD+GL50 groups by a double-blinded analysis, also showed that the MCD diet induced a significant increase of NAFLD activity, steatosis, and inflammation in livers of the MCD group, which were all markedly alleviated by GL treatment (Figure 1, E, F and G). Taken together, these results suggest that GL rescues apoptotic liver injury induced by MCD diet feeding, at least partially through directly inhibiting TNFα-induced hepatocyte apoptosis.

GL improves NASH-related liver fibrosis

Liver fibrosis is a hallmark of NAFLD progression to NASH. Masson Trichrome staining of collagen was used to measure liver fibrosis, and GL was found to significantly ameliorate NASH-associated collagen deposition induced by MCD diet feeding (Figure 2A). α-SMA is also another sensitive marker of liver fibrosis. MCD diet-induced upregulation of α-SMA expression was significantly decreased by GL treatment both at the protein level as determined by immunohistochemical staining (Figure 2B), and by mRNA analysis (Figure 2C). GL also significantly dampened the expression of fibrogenetic gene mRNAs including *Tgfb1*, *Timp1*, *Timp2*, *Cola1*, *Cola2*, *Mmp2* and *Mmp9* (Figure 2, D-J). These data demonstrate that GL significantly improves NASH-related liver fibrogenesis.

GL restores NASH-related hepatic lipids accumulation

In NASH, lipototoxicity caused by accumulating lipids in liver is a major trigger of liver toxicity (Fuchs and Sanyal, 2012). Therefore, effect of GL in MCD diet-induced lipid disruption was determined. When compared with control vehicle-treated MCD group, intraperitoneal injection of GL at 50 mg/kg significantly attenuated MCD diet-induced lipid accumulation in liver as revealed by Oil Red O staining (Figure 3A). When compared with the MCS group, liver TG and TC levels were both significantly increased in the MCD group, and both were significantly decreased by GL treatment (Figure 3, B and C). In contrast, serum TG and TC levels were significantly decreased after MCD diet feeding, which were also both normalized by GL treatment (Figure 3, D and E). Similarly, GL treatment also normalized MCD diet-induced disruption of serum HDL-cholesterol and LDL-cholesterol levels (Figure 3, F and G). These data strongly suggest that GL treatment could improve MCD diet-induced lipids disruption both in liver and serum.

Systematic lipids homeostasis is maintained by balanced mutual regulation of *de novo* lipids synthesis and lipids degradation by oxidation and subsequent ketogenesis (Tessari et al., 2009). To examine how GL restores MCD diet-induced dyslipidemia, lipid regulatory pathways were analyzed. When compared with MCS diet-fed mice, MCD diet-feeding significantly increased expression of *Lxr* and *Srebp1* mRNAs and the downstream lipids synthesis gene mRNA, *Fas*. Although GL treatment decreased the induction of *Lxr*, *Srebp1a* and *Srebp1c* mRNA, it showed no significant effect on the mRNA level of *Fas* and significantly restored MCD diet-decreased *Scd1* mRNA, both of which are encoded by two key lipogenic genes

(Figure 3H). Moreover, GL treatment significantly inhibited MCD diet-induced mRNA upregulation of the fatty acid transport gene mRNAs *Fatp3* and *Fatp4*, when compared with vehicle-treated MCD-fed mice (Figure 4H). MCD diet-feeding did not significantly change the expression of the ketogenesis pathway when compared with the MCS diet-fed group. In MCD diet-fed mice, GL treatment even significantly decreased *Acat1*, *Hmgcs, Hmgcl, Ppara and Cyp4a14* mRNA levels, and showed no significant effect in other mRNAs expression involved in ketogenesis and lipids oxidation, when compared with control vehicle treatment (Figure 3, I and J). These data indicate that GL may indirectly reduce lipogenesis by suppressing the expression of fatty acid transporters and not through enhancing lipid degradation via ketogenesis and oxidation.

GL decreases MCD-induced bile acids accumulation

Accompanied with the dysregulated lipids metabolism, bile acids are commonly accumulated in NASH both in mice and clinical patients (Bechmann et al., 2013; Gong et al., 2016; Arab et al., 2017). Several species of bile acids may exert direct toxic effects against hepatocytes and serve as danger molecules in triggering NLRP3 inflammasome activation (Gong et al., 2016; Hao et al., 2017). Thus, the effect of GL treatment on serum bile acids was examined under conditions of experimental NASH. MCD diet feeding significantly induced accumulation of free bile acids including α-MCA, β-MCA, CA, DCA, UDCA, and HDCA, by 2.9-, 12.1-, 18.0-, 3.7-, 7.6-, and 7.2-fold, respectively, all of which were markedly reduced by GL treatment (Figure 4A). Similarly, GL treatment significantly restored MCD diet-induced

serum accumulation of taurine-conjugated bile acids, T-β-MCA, T-CA, T-DCA, T-CDCA, T-UDCA and the glycine conjugated bile acids G-CA (Figure 4B). FXR activates the expression of small heterodimer partner 1 (SHP-1) that inhibits the liver receptor homolog 1(LRH-1) and represses expression of CYP7A1, which catalyzes the rate-limiting step in bile acid biosynthesis (Goodwin et al., 2000). Since the present study showed that all tested bile acids including the main primary bile acid, CA, were decreased by GL, GL treatment was inferred to influence the *de novo* synthesis of bile acids in liver. Therefore, FXR-SHP-CYP7A1 signaling, the predominant pathway for bile acids synthesis, was analyzed. In MCD diet-fed mice, hepatic FXR signaling was inhibited, and *Cyp7a1* mRNA was upregulated, when compared with MCS diet-fed mice. As expected, GL treatment significantly activated FXR, evidenced by upregulation of *Shp* mRNA and the downstream suppression of *Cyp7a1* mRNA, while *Fxr* mRNA itself was also significantly increased by GL treatment when compared with the vehicle-treated group in the mouse NASH model (Figure 4, C, D and E). In contrast, the bile acid export pump, *Bsep* mRNA was not significantly influenced by GL treatment (Figure 4F), suggesting a role of GL in inhibiting *de novo* bile acids synthesis.

To explain how GL could activate FXR in MCD diet-fed livers, the possibility that GL could act as a FXR ligand was explored. In mouse primary hepatocytes and HepG2 cells, no significant effect of FXR activation were found by neither GL nor GA treatment (Supplemental Figure 2, A and B) as well as GL-treated normal mice *in vivo* (Supplemental Figure 2C). Consistently, both GL and GA failed to activate FXR, while GW4064 induced FXR reporter

DMD Fast Forward. Published on June 29, 2018 as DOI: 10.1124/dmd.118.082008
This article has not been copyedited and formatted. The final version may differ from this version.

luciferase by 20-fold as a positive control in HepG2 cells (Supplemental Figure 2D), excluding GL as a direct FXR activator. These data prompted us to ask whether GL activated FXR only under NASH-related pathological conditions. Since NF- κB activation, a common pathological character under NASH condition, is known to lead to FXR inactivation (Wang et al., 2008)), rescue of FXR inactivation induced by NF- κB by GL was examined. LPS treatment slightly but significantly repressed FXR reporter activity, and both GL and GA treatment restored LPS-induced FXR inactivation (Supplemental Figure 2E). These data suggest that GL may restore bile acid homeostasis via attenuating the loss of FXR signaling induced by inflammatory damage.

GL inhibits NLRP3 inflammasome activation and meta-inflammation in mice

NLRP3 inflammasome activation is required for fibrosis development in NAFLD (Wree et al., 2014a; Wree et al., 2014b; Mridha et al., 2017). Activation of the NLRP3/inflammasome is a two-step process requiring a priming step (signal 1) induced by binding of damage-associated molecular patterns (DAMPs) or pathogen-associated molecular patterns (PAMPs) to receptors such as Toll-like receptor (TLR) to increase the transcription of NLRP3 and pro-IL-1β, followed by an activation step (signal 2) induced by the recruitment of ASC to activate the NLRP3 inflammasome to convert pro-caspase-1 into active caspase 1, which in turn processes pro-Il-1β into mature IL-1β (Guo et al., 2015). Since GL is a known inhibitor of the NLRP3 inflammasome (Honda et al., 2014), whether GL inhibited activation of the NLRP3 inflammasome in the NASH model was tested. When compared with MCS diet-fed mice, MCD

DMD Fast Forward. Published on June 29, 2018 as DOI: 10.1124/dmd.118.082008
This article has not been copyedited and formatted. The final version may differ from this version.

diet feeding induced a significant 2- to 4-fold increase of upstream *Tlr4*, *Tlr9*, and *Myd88* mRNAs, all of which were normalized by GL treatment (Figure 5, A, B and C). Similarly, MCD diet-induced *Casp1*, *Nlrp3*, and *Asc* mRNAs, by 5.5-, 4.8- and 7.7-fold, respectively, which were significantly reduced by GL treatment (Figure 5, D, E and F). These data suggest that GL could dampen the signal 1 activation of NLRP3/inflammasome in MCD diet-fed mice. Western blot analysis was performed to test the protein levels of pro-CASP1, active CASP-1, pro-IL-1β and active Il-1β. MCD diet induced upregulation of signal 1 and signal 2 when compared with MCS diet treatment. GL treatment decreased the protein expression of pro-CASP1 and pro-IL1β (Figure 5G), confirming GL's effect in inhibiting signal 1 of NLRP3 inflammasome activation. Furthermore, GL treatment was also found to inhibit the MCD diet-induced upregulation of active caspase1 (CASP1 p20) and cleaved IL-1β (Figure 5G). Additionally, GL significantly inhibited the upregulation of downstream proinflammatory cytokine mRNAs *Tnfa*, *Il6*, and *Il1b* (Figure 5, H, I and J) and serum release of IL-1β protein (Figure 5K), demonstrating a significantly improvement of NASH-related meta-inflammation by GL. These data demonstrate that GL treatment could dampen MCD diet-induced TLR/NLRP3 inflammasome activation and the related meta-inflammation.

Since previous reports and the present results indicate that bile acids accumulate in NASH and may be the main trigger for activation of the NLRP3 inflammsome (Arab et al., 2017; Hao et al., 2017), the possibility was explored whether GL could directly inhibit bile acid-induced NLRP3 inflammasome activation. Deoxycholic acid (DCA) was shown to induce NLRP3

inflammasome activation (Hao et al., 2017) and was thus used as a model to test GL's effect in inhibiting bile acid-induced NLRP3 inflammasome activation. In Raw 264.7 cells, both GL and GA significantly decreased DCA-induced upregulation of *Tnfa*, *Nlrp3*, and *Il1b* mRNAs (Figure 6). These data demonstrate that GL as well as its metabolite GA could directly suppress DCA-induced NLRP3 inflammasome activation *in vitro*, which at least partially explains GL's role in dampening MCD diet-induced NLRP3 inflammasome activation *in vivo*.

GA, the active metabolite of GL, improves MCD diet-induced liver injury

Structurally, GL is glycoside that hydrolyzed into its metabolite GA by intestinal bacteria after oral administration(Akao et al., 1994; Takeda et al., 1996). To test whether GA influences NASH, mice were treated with the MCD diet for 6 weeks, and then either intraperitoneally injected with GA (30 mg/kg) or intragastrically administered with GL by gavage (50 mg/kg) for an additional 3 weeks (Figure 7A). GA as well as GL gavage did not significantly change the body weight, liver weight, and liver index (Supplemental Figure 3). GA was found to significantly decrease the MCD diet-induced increase of ALT and AST levels (Figure 7, B and C). Similarly, GL gavage at a dose of 50 mg/kg also significantly ameliorated MCD diet-induced increase of serum ALT levels and AST levels (Figure 7, D and E). By histological analysis, 30 mg/kg of GA ameliorated MCD diet-induced hepatic steatosis (Figure 7, F and G). Similarly, GL gavage at a dose of 50 mg/kg improved the liver lipid overloading (Figure 7, H and I). These results indicate that GA may be required for the hepatoprotective effects of GL for the treatment of NASH.

DMD Fast Forward. Published on June 29, 2018 as DOI: 10.1124/dmd.118.082008
This article has not been copyedited and formatted. The final version may differ from this version.

Discussion

GL and its active metabolite GA have been demonstrated to be hepatoprotective, however, they have not been examined for their activities toward NASH. The current study shows that GL, via its activate metabolite GA, could decrease MCD diet-induced NASH, as revealed by improved hepatic steatosis, inflammation and fibrosis. Mechanistically, GL may restore NASH-induced dysregulation of bile acids and lipids and the resultant meta-inflammation.

Many factors such as cholesterol crystal (Duewell et al., 2010), ceramides (Chaurasia and Summers, 2015), and secondary bile acids (Hao et al., 2017) are known to accumulate in NASH livers and could act as DAMPS to induced NLRP3 inflammasome activation. Activation of the NLRP3 inflammasome results in the release of IL-1β, together with other pro-inflammatory cytokines such as TNFα, that trigger an inflammatory cascade that ultimately promotes pathological development of NASH. Thus, accumulated DAMPs, via activating NLRP3 inflammasome and other inflammatory pathways, may represent core pathological triggers in NASH development. In the present study using the MCD diet-induced NASH model, GL was shown to inhibit NLRP3 inflammasome activation accompanied by restoring abnormal serum bile acids accumulation, and GL could normalize the dysregulated lipids and bile acids and thereby reduce meta-inflammation. Since several bile acids are known to activate NLRP3/inflammasome signaling, GL may inhibit the NLRP3 inflammasome via the regulation of FXR signaling. However, GL did not activate FXR in normal mice *in vivo*, hepatocytes *in vitro* and failed to induce FXR reporter luciferase activity, indicating that GL is not a direct

FXR activator. FXR is known to have a reciprocal regulation with NF-κB activation (Wang et al., 2008). Under excessive inflammation, FXR signaling is reduced, resulting in the accumulation of bile acids and dysregulated lipid catabolism, which reciprocally triggers further inflammation (Bechmann et al., 2013). Although the exact mechanism warrants further clarification, the current study strongly indicates that GL and GA may target FXR mediated meta-inflammation in the treatment of NASH. The present data agree with a previous report that GL induces SHP expression and inhibits *Cyp7a1* expression in LCA-induced cholestatic liver injury model (Wang et al., 2012). Additionally, because the accumulation of bile acids may directly damage hepatocytes (Gumpricht et al., 2005), the observation that GL can restore bile acids homeostasis suggests that GL may be particularly suitable for the therapy of NASH featured with cholestasis.

In addition to restoration of the lipid and bile acid homeostasis, GL could also directly inhibit DCA-induced NLRP3 inflammasome activation, suggesting that it may target multiple nodes in treating NASH. In line with the present findings, GL was previously shown to inhibit NLRP3 inflammasome activation induced by diverse DAMPs or PAMPs in bone marrow-derived macrophages (Honda et al., 2014). MCC950, a NLRP3 selective inhibitor, was recently demonstrated to improve NAFLD pathology and fibrosis (Mridha et al., 2017), suggesting that the NLRP3 inflammasome might be a potential target for NASH therapy. Moreover, it was found that MCD diet-induced steatosis sensitized cholestatic liver injury and dysregulated bile acids synthesis and transport (Lionarons et al., 2016). The present results together with these

previous findings strongly indicate that dysregulated metabolism of lipids and bile acids and the resultant meta-inflammation is a pivotal event in NASH development.

GL by the oral route shows extremely low bioavailability (approximately 1%) and most of GL by oral intake is hydrolyzed into GA in the gut by intestinal bacteria, which is then absorbed and elicits its pharmacological effects(Nose et al., 1994; Yamamura et al., 1995; Takeda et al., 1996). In line with this point, GL gavage as well as direct GA i.p. injection could both combat experimental NASH, suggesting that effect of GL against MCD diet-induced NASH is largely through its primary metabolite GA. In contrast, GL but not GA, contributes to hepatoprotective effect of GL in ameliorating acetaminophen-induced liver injury (Yan et al., 2016). Thus, it is important to note that although both GL and GA have efficacy in various types of hepatic injury, the exact effects and thereby precise clinical applications of these agents need to be carefully considered.

In summary, the herbal medicine-derived compound GL may be a therapeutic option for NASH treatment, particularly that featured with cholestasis. Mechanistically, GL and/or GA may target bile acid-mediated meta-inflammation and block the reciprocal FXR-NLRP3 inflammasome pathway. All the data obtained from present MCD diet-induced NASH model demonstrate that GL and GA may be potentially effective against NASH. However, it is important to note that the MCD-diet induced NASH model, despite the presented liver steatosis and inflammation, does not show obesity, insulin resistance nor mimic aberrant increase of serum lipids, all of which are common pathophysiological characters of human NASH

DMD Fast Forward. Published on June 29, 2018 as DOI: 10.1124/dmd.118.082008
This article has not been copyedited and formatted. The final version may differ from this version.

(Hebbard and George, 2011). Thus, using long-term high-fat and/or high-sugar diet feeding model would help further confirm the translational potential of GL and GA in combating metabolic syndrome-related NASH.

DMD Fast Forward. Published on June 29, 2018 as DOI: 10.1124/dmd.118.082008
This article has not been copyedited and formatted. The final version may differ from this version.

Acknowledgments

We thank Grace L. Guo for providing us the PGL4-Shp-TK firefly luciferase construct and human FXR expression plasmid.

DMD Fast Forward. Published on June 29, 2018 as DOI: 10.1124/dmd.118.082008
This article has not been copyedited and formatted. The final version may differ from this version.

Authorship Contributions

Participated in research design: Yan, Hao, H. Wang, Gonzalez, G. Wang;

Conducted experiments: Yan, H. Wang, Q. Wang, Li, Takahashi, Yagai;

Contributed analytic tools or methods: Cao, Krausz;

Performed data analysis: Yan, H. Wang;

Wrote or contributed to the writing of the manuscript: Yan, Gonzalez, Hao.

References

Akao T, Hayashi T, Kobashi K, Kanaoka M, Kato H, Kobayashi M, Takeda S, and Oyama T (1994) Intestinal Bacterial Hydrolysis Is Indispensable to Absorption of 18-Beta-Glycyrrhetic Acid after Oral-Administration of Glycyrrhizin in Rats. *J Pharm Pharmacol* **46:**135-137.

Arab JP, Karpen SJ, Dawson PA, Arrese M, and Trauner M (2017) Bile acids and nonalcoholic fatty liver disease: Molecular insights and therapeutic perspectives. *Hepatology* **65:**350-362.

Bechmann LP, Kocabayoglu P, Sowa JP, Sydor S, Best J, Schlattjan M, Beilfuss A, Schmitt J, Hannivoort RA, Kilicarslan A, Rust C, Berr F, Tschopp O, Gerken G, Friedman SL, Geier A, and Canbay A (2013) Free fatty acids repress small heterodimer partner (SHP) activation and adiponectin counteracts bile acid-induced liver injury in superobese patients with nonalcoholic steatohepatitis. *Hepatology* **57:**1394-1406.

Chaurasia B and Summers SA (2015) Ceramides - Lipotoxic Inducers of Metabolic Disorders. *Trends Endocrinol Metab* **26:**538-550.

Duewell P, Kono H, Rayner KJ, Sirois CM, Vladimer G, Bauernfeind FG, Abela GS, Franchi L, Nunez G, Schnurr M, Espevik T, Lien E, Fitzgerald KA, Rock KL, Moore KJ, Wright SD, Hornung V, and Latz E (2010) NLRP3 inflammasomes are required for atherogenesis and activated by cholesterol crystals. *Nature* **464:**1357-1361.

Feldstein AE, Canbay A, Angulo P, Taniai M, Burgart LJ, Lindor KD, and Gores GJ (2003) Hepatocyte apoptosis and fas expression are prominent features of human nonalcoholic steatohepatitis. *Gastroenterology* **125:**437-443.

Fuchs M and Sanyal AJ (2012) Lipotoxicity in NASH. *J Hepatol* **56:**291-293.

Gong Z, Zhou J, Zhao S, Tian C, Wang P, Xu C, Chen Y, Cai W, and Wu J (2016) Chenodeoxycholic acid activates NLRP3 inflammasome and contributes to cholestatic liver fibrosis. *Oncotarget* **7:**83951-83963.

Goodwin B, Jones SA, Price RR, Watson MA, McKee DD, Moore LB, Galardi C, Wilson JG, Lewis MC, Roth ME, Maloney PR, Willson TM, and Kliewer SA (2000) A regulatory cascade of the nuclear receptors FXR, SHP-1, and LRH-1 represses bile acid biosynthesis. *Mol Cell* **6:**517-526.

Gumpricht E, Dahl R, Devereaux MW, and Sokol RJ (2005) Licorice compounds glycyrrhizin and 18beta-glycyrrhetinic acid are potent modulators of bile acid-induced cytotoxicity in rat hepatocytes. *J Biol Chem* **280:**10556-10563.

Guo H, Callaway JB, and Ting JP (2015) Inflammasomes: mechanism of action, role in disease, and therapeutics. *Nat Med* **21:**677-687.

Hao H, Cao L, Jiang C, Che Y, Zhang S, Takahashi S, Wang G, and Gonzalez FJ (2017) Farnesoid X Receptor Regulation of the NLRP3 Inflammasome Underlies Cholestasis-Associated Sepsis. *Cell Metab* **25:**856-867 e855.

Hebbard L and George J (2011) Animal models of nonalcoholic fatty liver disease. *Nat Rev Gastroenterol Hepatol* **8:**35-44.

Honda H, Nagai Y, Matsunaga T, Okamoto N, Watanabe Y, Tsuneyama K, Hayashi H, Fujii I, Ikutani M, Hirai Y, Muraguchi A, and Takatsu K (2014) Isoliquiritigenin is a potent inhibitor of NLRP3 inflammasome activation and diet-induced adipose tissue inflammation. *J Leukocyte Biol* **96:**1087-1100.

Jadeja R, Devkar RV, and Nammi S (2014) Herbal medicines for the treatment of nonalcoholic steatohepatitis: current scenario and future prospects. *Evid Based Complement Alternat Med* **2014:**648308.

Leist M, Gantner F, Bohlinger I, Germann PG, Tiegs G, and Wendel A (1994) Murine hepatocyte apoptosis induced in vitro and in vivo by TNF-alpha requires transcriptional arrest. *J Immunol* **153:**1778-1788.

Li JY, Cao HY, Liu P, Cheng GH, and Sun MY (2014) Glycyrrhizic acid in the treatment of liver diseases: literature review. *Biomed Res Int* **2014:**872139.

Lionarons DA, Heger M, van Golen RF, Alles LK, van der Mark VA, Kloek JJ, de Waart DR, Marsman HA, Rusch H, Verheij J, Beuers U, Paulusma CC, and van Gulik TM (2016) Simple steatosis sensitizes cholestatic rats to liver injury and dysregulates bile salt synthesis and transport. *Sci Rep* **6:**31829.

Mridha AR, Wree A, Robertson AAB, Yeh MM, Johnson CD, Van Rooyen DM, Haczeyni F, Teoh NC, Savard C, Ioannou GN, Masters SL, Schroder K, Cooper MA, Feldstein AE, and Farrell GC (2017) NLRP3 inflammasome blockade reduces liver inflammation and fibrosis in experimental NASH in mice. *J Hepatol* **66:**1037-1046.

Nose M, Ito M, Kamimura K, Shimizu M, and Ogihara Y (1994) A Comparison of the Antihepatotoxic Activity between Glycyrrhizin and Glycyrrhetinic Acid. *Planta Med* **60:**136-139.

Osborn O and Olefsky JM (2012) The cellular and signaling networks linking the immune system and metabolism in disease. *Nat Med* **18:**363-374.

Schoemaker MH, Gommans WA, Conde de la Rosa L, Homan M, Klok P, Trautwein C, van Goor H, Poelstra K, Haisma HJ, Jansen PLM, and Moshage H (2003) Resistance of rat hepatocytes against bile acid-induced apoptosis in cholestatic liver injury is due to nuclear factor-kappa B activation. *Journal of Hepatology* **39:**153-161.

Takeda S, Ishihara K, Wakui Y, Amagaya S, Maruno M, Akao T, and Kobashi K (1996) Bioavailability study of glycyrrhetic acid after oral administration of glycyrrhizin in rats; Relevance to the intestinal bacterial hydrolysis. *J Pharm Pharmacol* **48:**902-905.

Tessari P, Coracina A, Cosma A, and Tiengo A (2009) Hepatic lipid metabolism and non-alcoholic fatty liver disease. *Nutr Metab Cardiovasc Dis* **19:**291-302.

Wang CY, Mayo MW, and Baldwin AS, Jr. (1996) TNF- and cancer therapy-induced apoptosis: potentiation by inhibition of NF-kappaB. *Science* **274:**784-787.

Wang H, Fang ZZ, Meng R, Cao YF, Tanaka N, Krausz KW, and Gonzalez FJ (2017) Glycyrrhizin and glycyrrhetinic acid inhibits alpha-naphthyl isothiocyanate-induced liver injury and bile acid cycle disruption. *Toxicology* **386:**133-142.

Wang YD, Chen WD, Wang MH, Yu DN, Forman BM, and Huang WD (2008) Farnesoid X Receptor Antagonizes Nuclear Factor kappa B in Hepatic Inflammatory Response. *Hepatology* **48:**1632-1643.

Wang YG, Zhou JM, Ma ZC, Li H, Liang QD, Tan HL, Xiao CR, Zhang BL, and Gao Y (2012) Pregnane X receptor mediated-transcription regulation of CYP3A by glycyrrhizin: a possible mechanism for its hepatoprotective property against lithocholic acid-induced injury. *Chem Biol Interact* **200:**11-20.

Wong CR, Nguyen MH, and Lim JK (2016) Hepatocellular carcinoma in patients with non-alcoholic fatty liver disease. *World J Gastroenterol* **22:**8294-8303.

Wong RJ, Cheung R, and Ahmed A (2014) Nonalcoholic steatohepatitis is the most rapidly growing indication for liver transplantation in patients with hepatocellular carcinoma in the U.S. *Hepatology* **59:**2188-2195.

Wree A, Eguchi A, McGeough MD, Pena CA, Johnson CD, Canbay A, Hoffman HM, and Feldstein AE (2014a) NLRP3 inflammasome activation results in hepatocyte pyroptosis, liver inflammation, and fibrosis in mice. *Hepatology* **59:**898-910.

Wree A, McGeough MD, Pena CA, Schlattjan M, Li HY, Inzaugarat ME, Messer K, Canbay A, Hoffman HM, and Feldstein AE (2014b) NLRP3 inflammasome activation is required for fibrosis development in NAFLD. *J Mol Med* **92:**1069-1082.

Wu X, Zhang L, Gurley E, Studer E, Shang J, Wang T, Wang C, Yan M, Jiang Z, Hylemon PB, Sanyal AJ, Pandak WM, Jr., and Zhou H (2008) Prevention of free fatty acid-induced

hepatic lipotoxicity by 18beta-glycyrrhetinic acid through lysosomal and mitochondrial pathways. *Hepatology* **47:**1905-1915.

Xie G, Wang X, Huang F, Zhao A, Chen W, Yan J, Zhang Y, Lei S, Ge K, Zheng X, Liu J, Su M, Liu P, and Jia W (2016) Dysregulated hepatic bile acids collaboratively promote liver carcinogenesis. *Int J Cancer* **139:**1764-1775.

Yamamura Y, Santa T, Kotaki H, Uchino K, Sawada Y, and Iga T (1995) Administration-route dependency of absorption of glycyrrhizin in rats: intraperitoneal administration dramatically enhanced bioavailability. *Biol Pharm Bull* **18:**337-341.

Yan T, Wang H, Zhao M, Yagai T, Chai Y, Krausz KW, Xie C, Cheng X, Zhang J, Che Y, Li F, Wu Y, Brocker CN, Gonzalez FJ, Wang G, and Hao H (2016) Glycyrrhizin Protects against Acetaminophen-Induced Acute Liver Injury via Alleviating Tumor Necrosis Factor alpha-Mediated Apoptosis. *Drug Metab Dispos* **44:**720-731.

Younossi ZM, Koenig AB, Abdelatif D, Fazel Y, Henry L, and Wymer M (2016) Global epidemiology of nonalcoholic fatty liver disease-Meta-analytic assessment of prevalence, incidence, and outcomes. *Hepatology* **64:**73-84.

Zhang L and Schuppan D (2014) Traditional Chinese Medicine (TCM) for fibrotic liver disease: hope and hype. *J Hepatol* **61:**166-168.

Zhou L, Song Y, Zhao J, Qin H, Zhang G, Zhou Y, and Wu X (2016) Monoammonium glycyrrhizinate protects rifampicin- and isoniazid-induced hepatotoxicity via regulating the expression of transporter Mrp2, Ntcp, and Oatp1a4 in liver. *Pharm Biol* **54:**931-937.

Zoller H and Tilg H (2016) Nonalcoholic fatty liver disease and hepatocellular carcinoma. *Metabolism* **65:**1151-1160.

Footnotes

This research was supported by National Natural Science Foundation of China (grants 81430091, 81720108032, 81421005, 91429308 and 81603194), the Project for Major New Drug Innovation and Development (grant 2015ZX09501010); and Overseas Expertise Introduction Project for Discipline Innovation (G20582017001) and China Postdoctoral Science Foundation (grants 2016M600455 and 2017T100423), and the National Cancer Institute Intramural Research Program.

Figure Legends

Figure 1. Glycyrrhizin significantly alleviates MCD diet-induced liver damage, improves TUNEL staining, and reduces serum transaminases.

(A), Mouse experiment procedure scheme. (B), H & E-staining of liver sections, original magnification: 20×; Scale bar, 50 μm. (C) TUNEL-staining analysis of paraffin-embedded livers, original magnification: 20×; Scale bar, 50 μm. (D), Serum ALT levels. (E, F and G), NAFLD scoring statistics for H&E slides. Data are presented as means ± SD. Statistic differences between experimental groups were determined by two-tailed Student's *t* test. n=6-8 for each group. MCS, MCS diet-fed mice treated with saline; MCS+GL50, MCS diet-fed mice treated with 50 mg/kg of GL. MCD, MCD diet-fed mice treated with saline; MCD+GL50, MCD diet-fed mice treated with 50 mg/kg of GL. ###p<0.001 versus MCS group. **p<0.01 and ***p<0.001 versus MCD group.

Figure 2. Glycyrrhizin significantly dampens MCD-induced liver fibrogenesis. (A and B), Masson's Trichrome staining (A) and immunohistochemistry staining of α-SMA (B) for paraffin-embed livers, original magnification: 20X; scale bar, 50 μm. (C, D, E, and F), levels of α*Sma*, *Tgfb1*, *Timp1* and *Timp2* mRNAs in livers. (F, G, H, I and J), *Cola1*, *Cola2*, *Mmp2* and *Mmp9* mRNAs in livers. Data are presented as means ± SD. Statistic differences between experimental groups were determined by two-tailed Student's *t* test. n=6-8 in each group. MCS, MCS diet-fed mice treated with saline; MCD, MCD diet-fed mice treated with saline;

MCD+GL50, MCD diet-fed mice treated with 50 mg/kg of GL. ##p<0.01 and ###p<0.001 versus MCS group. *p<0.05, **p<0.01 and ***p<0.001 versus MCD group.

Figure 3. Glycyrrhizin significantly reduces MCD-induced lipids accumulation in liver via inhibiting fatty acid uptake. (A) Oil Red O-staining of liver sections, original magnification: 20×; scale bar, 50 μm. (B and C), Liver TG and TC levels. (D and E), Serum TG and TC levels. (F and G), Serum HDL-cholesterol and LDL-cholesterol levels. (H-J), Effect of GL in the mRNA expression involved in the pathway of lipogenesis (H), ketogenesis (I), and beta-oxidation (J). Data are presented as means ± SD. Statistic differences between experimental groups were determined by two-tailed Student's *t* test. n=6-8 in each group. MCS, MCS diet-fed mice treated with saline; MCD, MCD diet-fed mice treated with saline; MCD+GL50, MCD diet-fed mice treated with 50 mg/kg of GL. #p<0.05; ##p<0.01 and ###p<0.001 versus MCS group. *p<0.05, **p<0.01 and ***p<0.001 versus MCD group.

Figure 4. Glycyrrhizin activates liver FXR/SHP/CYP7A1 signaling and rescues MCD-induced bile acids disruption. (A), Serum level of free bile acids, α-MCA, β-MCA, CA, DCA, UDCA and HDCA. (B), Serum level of conjugated bile acids, T-β-MCA, T-CA, T-DCA, T-CDCA, T-UDCA, T-HDCA and G-CA. (C, D, E and C), hepatic mRNA levels of *Fxr*, *Shp*, *Cyp7a1* and *Bsep*. Data are presented as means ± SD. Statistic differences between experimental groups were determined by two-tailed Student's *t* test. n=6-8 in each group. MCS, MCS diet-fed mice treated with saline; MCD, MCD diet-fed mice treated with saline;

MCD+GL50, MCD diet-fed mice treated with 50 mg/kg of GL. #p<0.05; ##p<0.01 and ###p<0.001 versus MCS group. *p<0.05, **p<0.01 and ***p<0.001 versus MCD group.

Figure 5. Glycyrrhizin significantly reduces MCD-induced TLR/NLRP3 inflammasome activation and the related meta-inflammation. (A, B and C), *Tlr4*, *Tlr9* and *Myd88* mRNA levels in livers. (D, E and F), mRNA levels of *Nlrp3*, *Casp1 and Asc* in livers. (G), Western blot analysis of pro-CASP1, cleaved CASP1, pro-IL1β, and cleaved IL1β in livers. (H, I and J), mRNA levels of proinflammatory cytokines, *Tnfa*, *Il6*, and *Il1b* in livers. (K), Elisa analysis of serum Il-1β level in mice. Data are presented as means ± SD. Statistic differences between experimental groups were determined by two-tailed Student's *t* test. n=6-8 in each group. MCS, MCS diet-fed mice treated with saline; MCD, MCD diet-fed mice treated with saline; MCD+GL50 or MCD+GL, MCD diet-fed mice treated with 50 mg/kg of GL. #p<0.05; ##p<0.01 and ###p<0.001 versus MCS group. *p<0.05, **p<0.01 and ***p<0.001 versus MCD group.

Figure 6. Both GL and GA significantly inhibit DCA-induced *Tnfa*, *Nlrp3*, and *Il1b* mRNA. (A, B and C), Effect of GL in DCA-induced mRNA of *Tnfa*, *Nlrp3*, and *Il1b* mRNAs in Raw 264.7 cells. (D, E and F), Effect of GA in DCA-induced *Tnfa*, *Nlrp3*, and *I11b* mRNAs in Raw 264.7 cells. Data are presented as means ± SD. Statistic differences determined by one-way ANOVA followed by Dunnett's multiple comparisons test among multiple-group comparisons. n=3 per group. Raw 264.7 cells were pretreated with 0.1% DMSO, GL or GA for 30 minutes, and then treated with 200 μM of DCA for additional four hours to further perform

mRNA analysis. DMSO, 0.1% DMSO/vehicle-treated control vehicle group; DCA, 0.1% DMSO/DCA-treated group; DCA+GL50, 50 μM of GL/DCA-treated group; DCA+GL250, 250 μM of GL/DCA-treated group; DCA+GA3, 3 μM of GA/DCA-treated group; DCA+GA6, 6 μM of GA/DCA-treated group. # $p<0.05$; ##$p<0.01$ and ###$p<0.001$ versus DMSO group. *$p<0.05$, **$p<0.01$ and ***$p<0.001$ versus DCA group.

Figure 7. GL's active metabolite, GA, significantly reduces MCD-induced liver injury. (A), Mouse experiment procedure scheme. (B and C), Serum ALT and AST levels in saline or GA-treated mice. (D and E), Serum ALT and AST levels in saline or GL gavage-treated mice. (F and G), Representative H&E staining (F) and Oil Red O staining (G) for livers from MCD group and MCD+GA30 group; (H and I), Representative H&E staining (H) and Oil Red O staining (I) for livers from MCD group and MCD+GL50 (po) group. Original magnification: 20×; Scale bar, 50 μm. Data are presented as means ± SD. Statistic differences between experimental groups were determined by two-tailed Student's *t* test. n=5 in each group. MCS, MCS diet-fed mice treated with saline; MCD, MCD diet-fed mice treated with saline; MCD+GA30, MCD diet-fed mice treated with 30 mg/kg of GA by intraperitoneal injection; MCD+GL50 (p.o.), MCD diet-fed mice treated with 50 mg/kg of GL by gavage. #$p<0.05$; ##$p<0.01$ and ###$p<0.001$ versus MCS group. *$p<0.05$, **$p<0.01$ and ***$p<0.001$ versus MCD group.

DMD Fast Forward. Published on June 29, 2018 as DOI: 10.1124/dmd.118.082008
This article has not been copyedited and formatted. The final version may differ from this version.

Figures

Figure 1

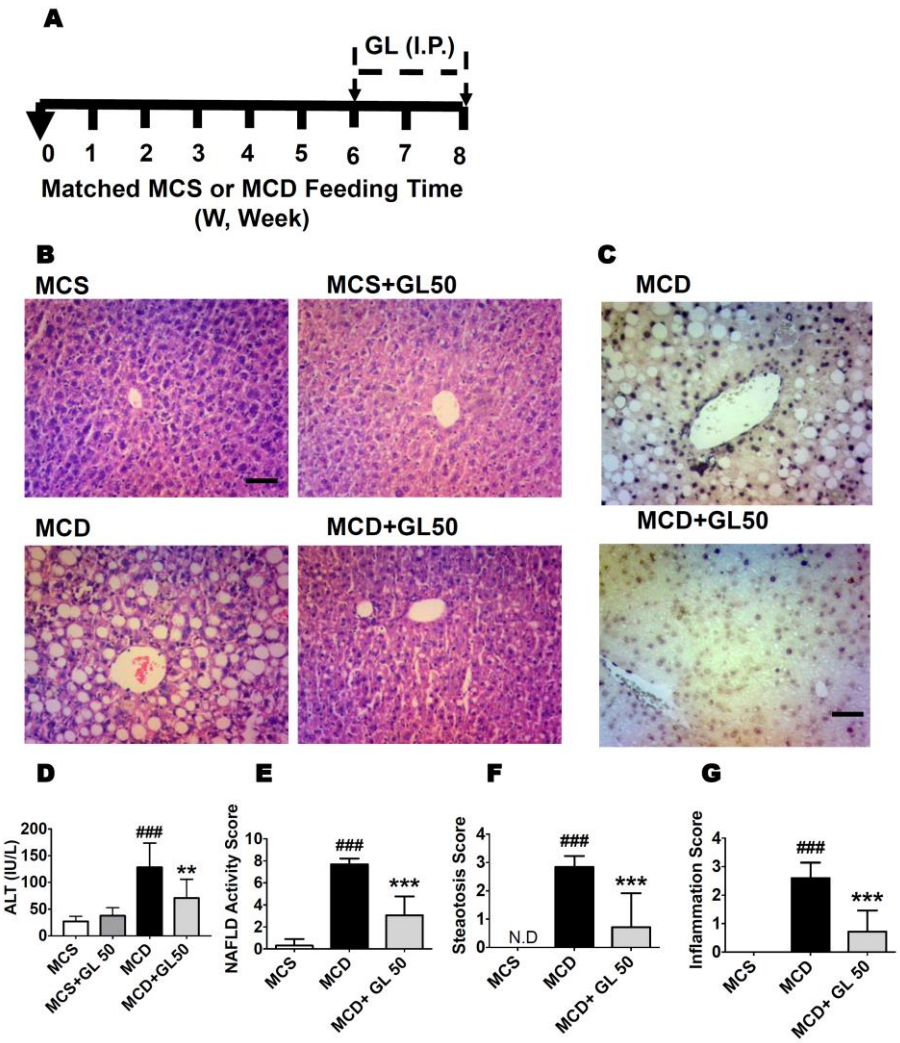

DMD Fast Forward. Published on June 29, 2018 as DOI: 10.1124/dmd.118.082008
This article has not been copyedited and formatted. The final version may differ from this version.

Figure 2

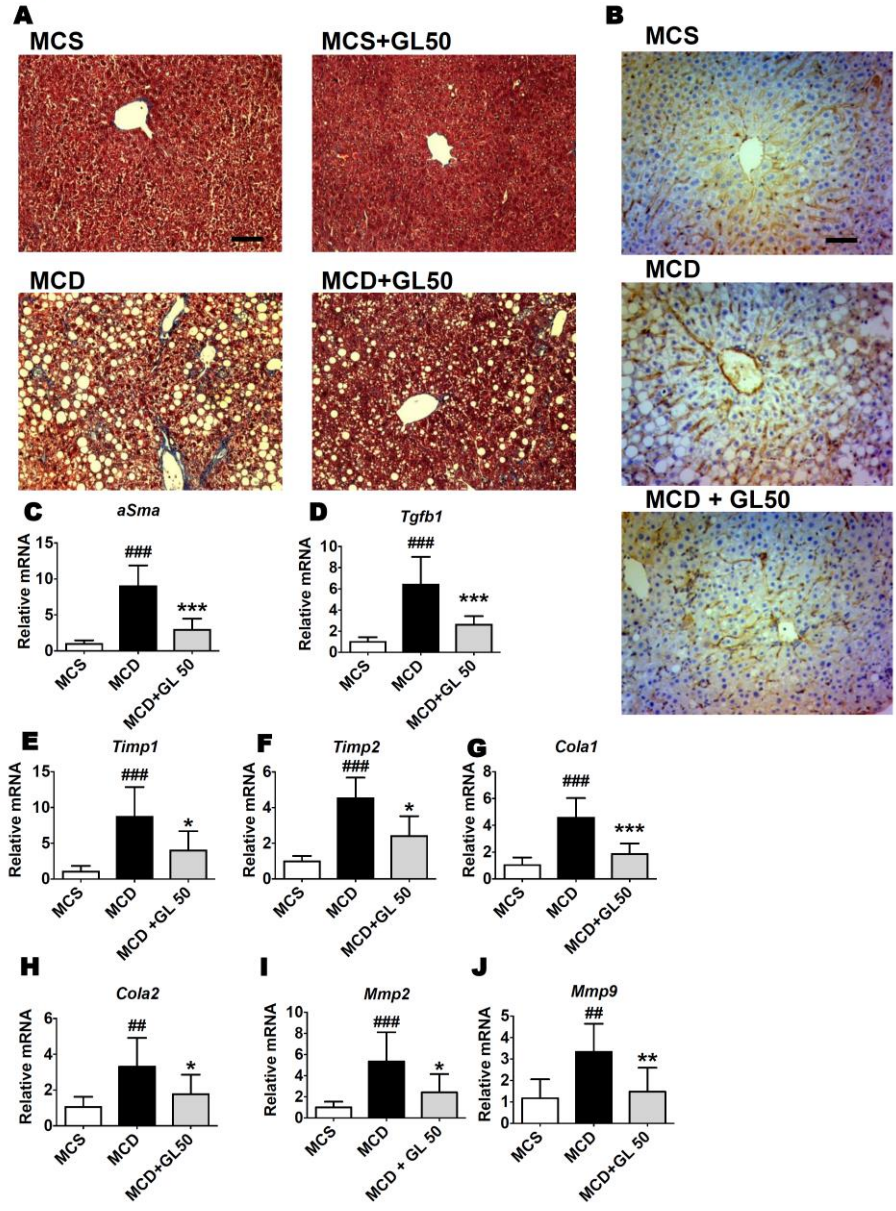

DMD Fast Forward. Published on June 29, 2018 as DOI: 10.1124/dmd.118.082008
This article has not been copyedited and formatted. The final version may differ from this version.

Figure 3

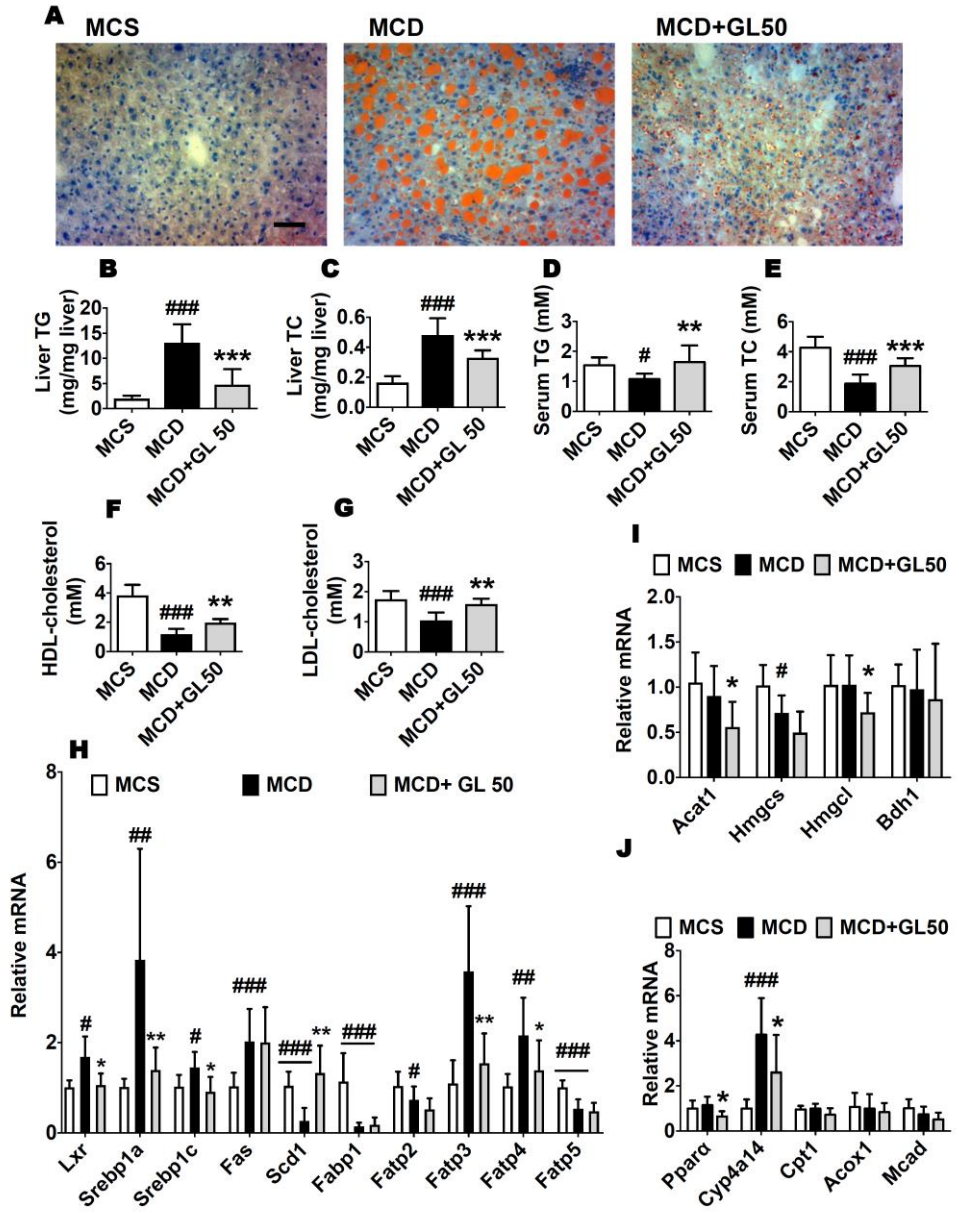

DMD Fast Forward. Published on June 29, 2018 as DOI: 10.1124/dmd.118.082008
This article has not been copyedited and formatted. The final version may differ from this version.

Figure 4

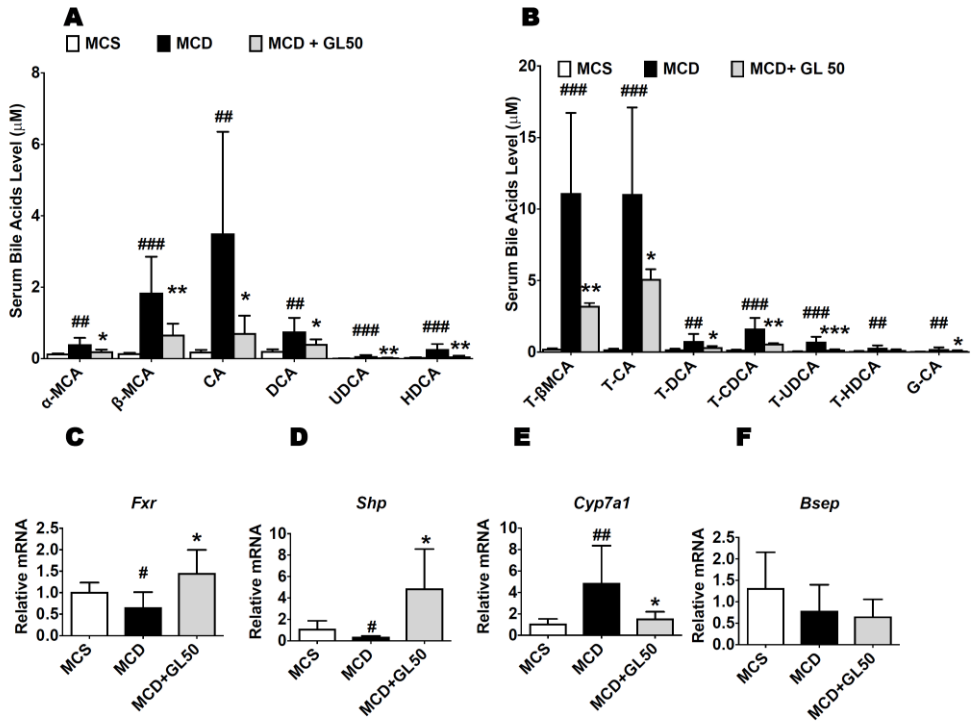

DMD Fast Forward. Published on June 29, 2018 as DOI: 10.1124/dmd.118.082008
This article has not been copyedited and formatted. The final version may differ from this version.

Figure 5

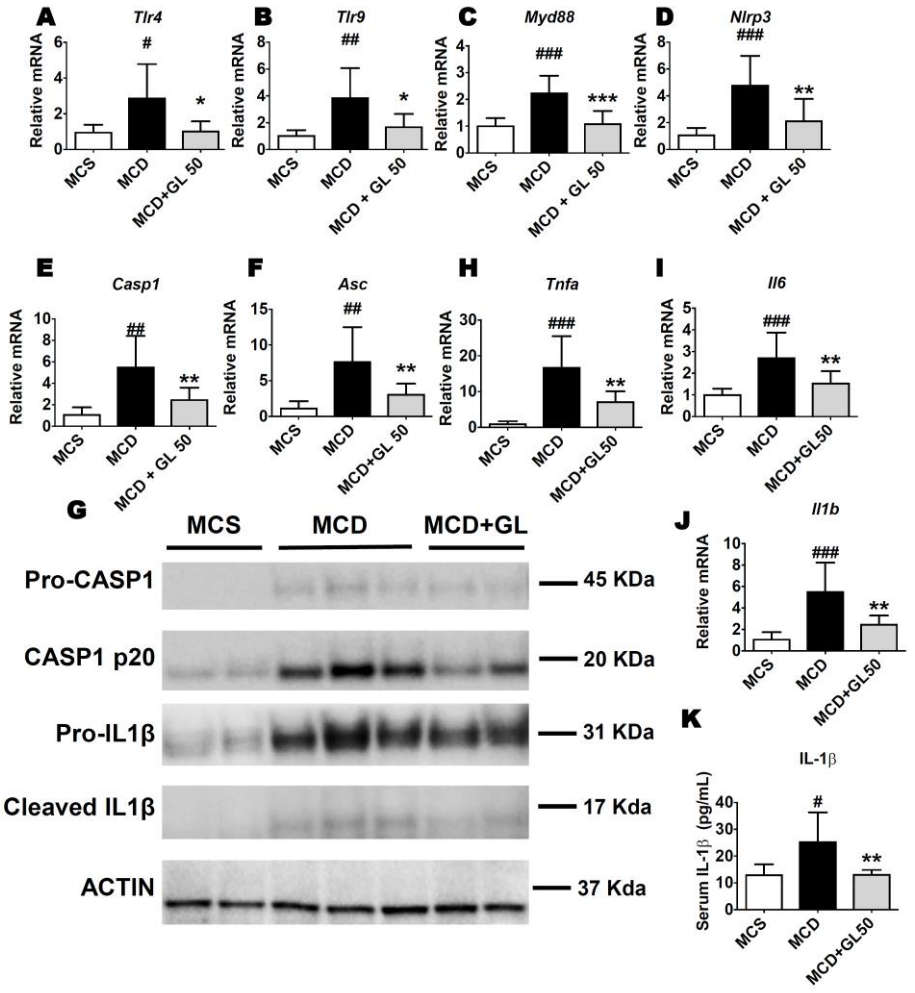

DMD Fast Forward. Published on June 29, 2018 as DOI: 10.1124/dmd.118.082008
This article has not been copyedited and formatted. The final version may differ from this version.

Figure 6

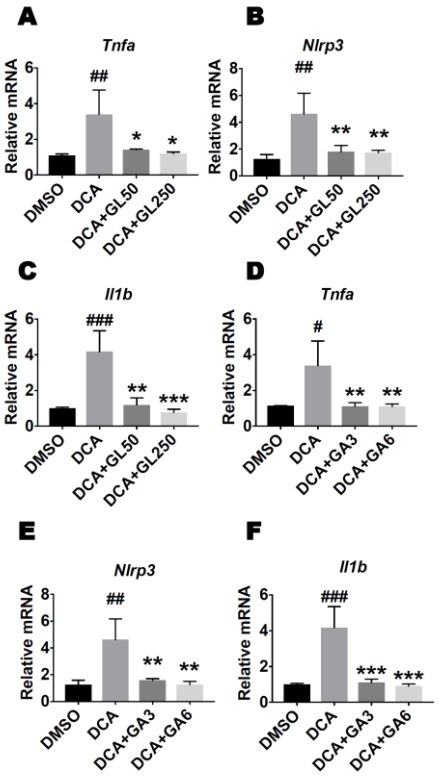

DMD Fast Forward. Published on June 29, 2018 as DOI: 10.1124/dmd.118.082008
This article has not been copyedited and formatted. The final version may differ from this version.

Figure 7

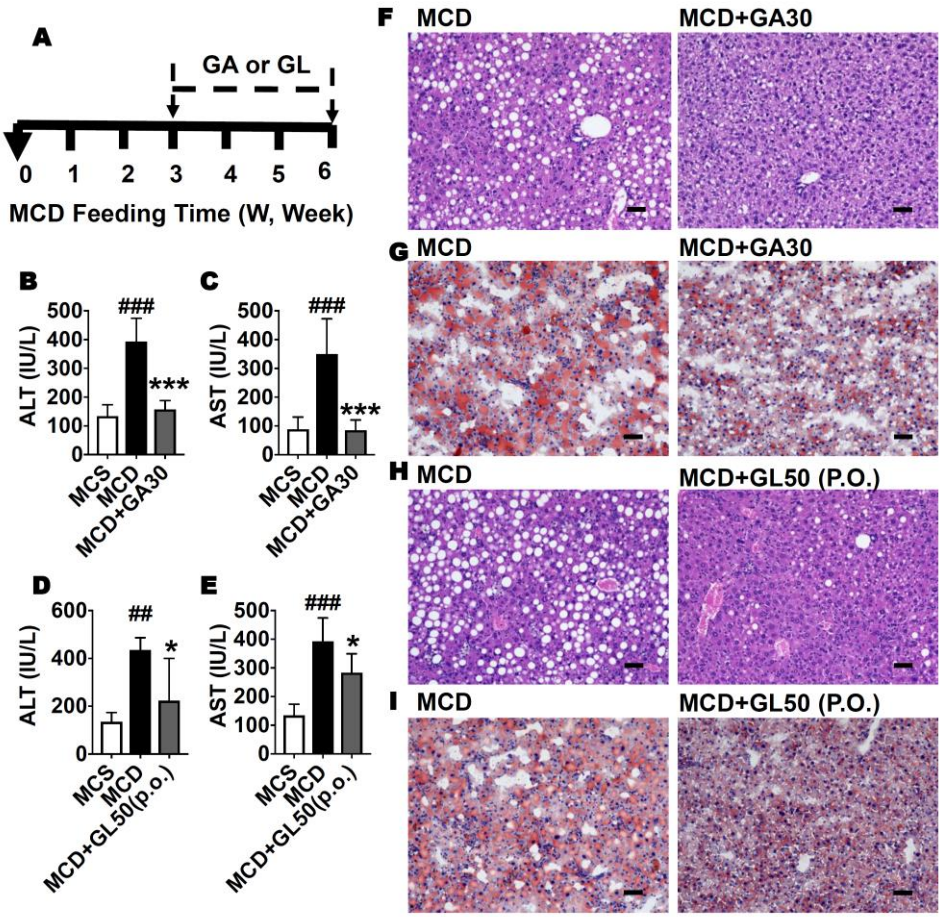

Supplemental Data

Title: Glycyrrhizin alleviates non-alcoholic steatohepatitis via modulating bile acids and meta-inflammation

Authors: Tingting Yan, Hong Wang, Lijuan Cao, Qiong Wang, Shogo Takahashi, Tomoki Yagai, Guolin Li, Kristopher W. Krausz, Guangji Wang, Frank J. Gonzalez, Haiping Hao.

Journal Title: Drug Metabolism and Disposition

Supplemental Figure 1

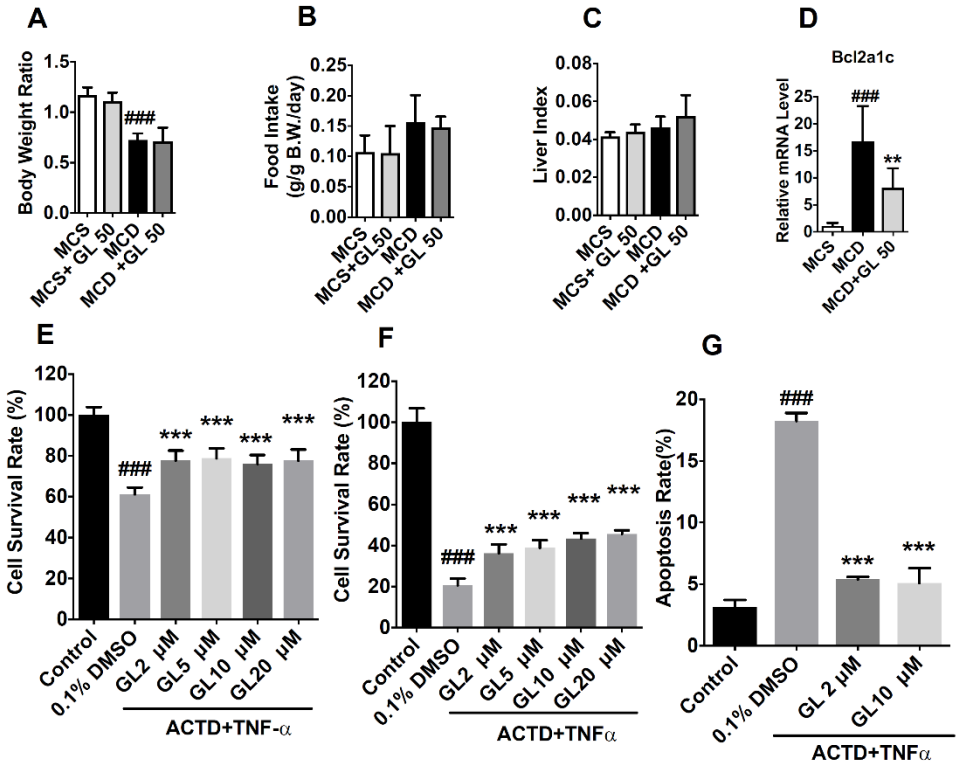

Supplemental Figure 1. GL decreases MCD-induced apoptotic signaling activation, while shows no significant effect in MCD-induced body weight loss, food intake, and liver index. (A), Body weight ratio, the ratio of body weight at the end of experiment to body weight before MCD diet feeding. (B), Average food intake record for the first week after GL injection, all mice were single-caged and food intake was recorded every day for 7 days. (C), Liver index, ratio of liver weight to body weight. (D), Levels of liver apoptotic signaling, Bcl2a1c mRNAs. (E and F), GL treatment alleviates ACTD/TNFα-induced HepG2 cell death at 13 h (E) and 24 h (F) after TNFα challenge by CKK-8 kit. (G), GL treatment alleviates ACTD/TNFα-induced HepG2 apoptosis by FACS assay at 13 h after TNFα challenge. Data are presented as means ± SD. Statistic

differences determined by one-way ANOVA followed by Dunnett's multiple comparisons test among multiple-group comparisons. For mouse experiments, n=6-8 in each group. Bcl2a1c, B-cell leukemia/lymphoma 2 related protein a1c. MCS, MCS diet-fed mice treated with saline; MCD, MCD diet-fed mice treated with saline; MCD+GL50, MCD diet-fed mice treated with 50 mg/kg of GL. ###$p<0.001$ versus MCS group. *$p<0.05$ and **$p<0.01$ versus MCD group. For cell culture experiments, HepG2 cells were pretreated with 0.1% DMSO or various concentration of GL for 30 minutes in the presence or absence of 0.3 μM of ACTD, and then 30 ng/mL of recombinant human TNFα were added to induce cell death. CCK-8 kit assay or FACS assay was performed at 13 h or 24 h after TNFα treatment to test the cell viability. n=6-12 for F and G, and n=3 for H. ###$p<0.001$ versus control group. ***$p<0.001$ versus 0.1% DMSO group.

Supplemental Figure 2

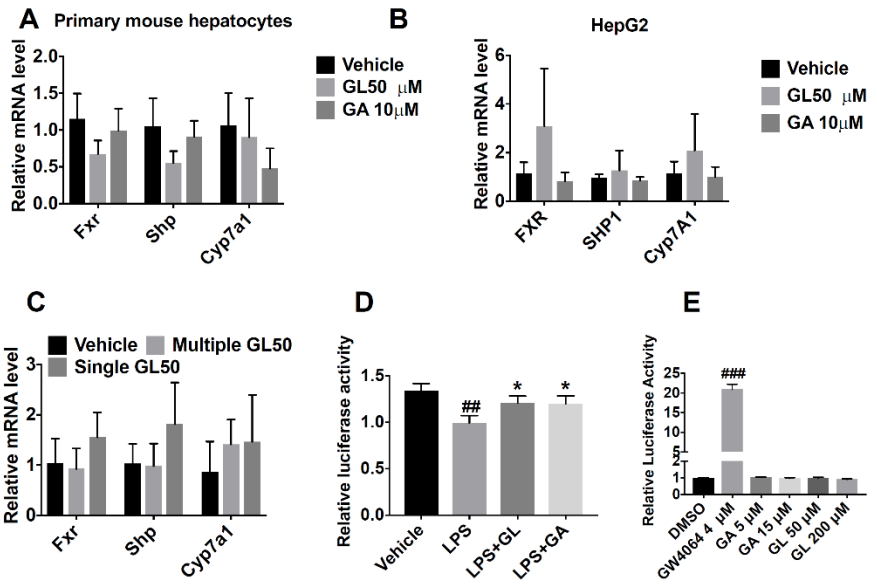

Supplemental Figure 2. Effect of GL in FXR activation *in vivo* and *in vitro*. (A-C), Effect of GL in the mRNA expression of FXR target genes in primary mouse hepatocytes (A), HepG2 cells (B), and in mice (C). Primary hepatocytes isolated from 8-week old male mice or HepG2 cells were treated with 50 μM of GL, 10 μM of GA or control vehicle 0.1% DMSO (n=3-6 per group) for 24 h in 10% DMEM culture medium; mice were treated with control vehicle (Vehicle group), 50 mg/kg of GL for a single injection (Single GL50 group) or 7 consecutive days (Multiple GL50 group), and then livers were collected for mRNA analysis at the end of experiments, n=5 mice in each group. (D), Effect of 200 μM of GL and 15 μM of GA in LPS-induced FXR inactivation in HepG2 cells. (E), Effect of 50 μM or 200 μM of GL, 5 μM or 15 μM of GA, 4 μM of GW4064 in the FXR luciferase reporter activity; HepG2 cells in 10% DMEM culture medium (n=3 per group). Data are presented as means ± SD. Statistic differences determined by one-way ANOVA followed by Dunnett's multiple comparisons test among multiple-group comparisons. #p<0.05; ##p<0.01 and ###p<0.001 versus control vehicle-treated group. *p<0.05 versus LPS-treated group.

Supplemental Figure 3

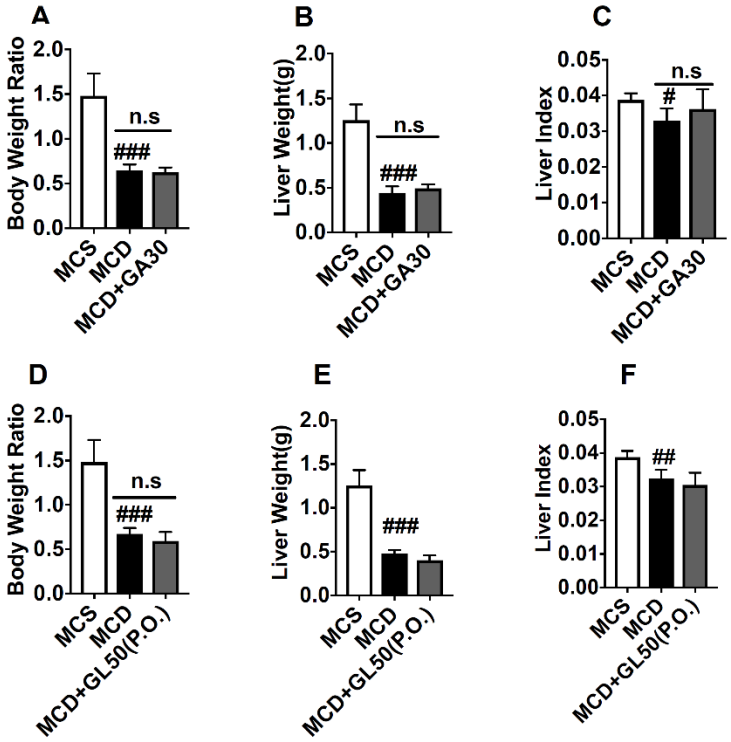

Supplemental Figure 3. GA as well as GL gavage shows no significant effect in body weight, liver weight, and liver index. (A), Body weight ratio, the ratio of body weight at the end of experiment to body weight at Day 0 of the experiment. (B), Liver weight. (C), Liver index, ratio of liver weight to body weight. (D), Body weight ratio, the ratio of body weight at the end of experiment to body weight at Day 0 of the experiment. (E), liver weight. (F), Liver index, ratio of liver weight to body weight. Data are presented as means ± SD. Statistic differences determined by one-way ANOVA followed by Dunnett's multiple comparisons test among multiple-group comparisons. #$p<0.05$; ##$p<0.01$ and ###$p<0.001$ versus MCS group. n=5 in each group. MCS, MCS diet-fed mice treated with saline; MCD, MCD diet-fed mice treated with saline;

MCD+GL50(P.O.), MCD diet-fed mice treated with 50 mg/kg of GL by gavage. MCD+GA30, MCD diet-fed mice treated with 30 mg/kg of GA.